Trees (2010) 24:609–619
DOI 10.1007/s00468-010-0431-z

ORIGINAL PAPER

# Using terrestrial laser scanner for estimating leaf areas of individual trees in a conifer forest

**Peng Huang · Hans Pretzsch**

Received: 29 April 2009 / Revised: 20 October 2009 / Accepted: 11 March 2010 / Published online: 30 March 2010


**Abstract** A method that applies the terrestrial laser scanning to estimate leaf areas of individual trees in a mature conifer forest is presented. It is based on the theory of conventional optical LAI determinations, but refined for the inclusion of 3D depth information from the laser scanner. For each objective tree, we first used a single scan to measure local gap fractions beyond determined crown depths and combined this scan with other scans to delineate the geometrical dimensions of the crown. Then, through integrating the information from both aspects, the local leaf area density and the corresponding volume were derived. Finally, the total leaf area was obtained as the scalar product of these two variables. As most procedures were implemented on segmented 2D range images, the method possesses high efficiency. Additionally, through using gap fraction beyond determined crown depths, it solved the zero gap fraction problem encountered in segmented hemispherical photograph analysis. The method was tested on 11 trees in a 39 years old Norway spruce (*Picea abies* [L.] Karst.) stand located in southern Bavaria, Germany. Through correlation of the results with the estimates obtained with allometric equations, the accuracy was validated. The influence of the crown depth, for measuring gap fraction, and the segment size on estimation were also analyzed.

Communicated by W. Bilger.

P. Huang (✉) · H. Pretzsch
Chair for Forest Growth and Yield Science,
Department of Ecology and Landscape Management,
Technical University of Munich, Am Hochanger 13,
85354 Freising, Germany
e-mail: Peng.Huang@lrz.tu-muenchen.de

**Keywords** Leaf area · Gap fraction · Norway spruce · Lidar · Allometry

## Introduction

The leaf area per unit area, namely leaf area index (LAI), has always been one of the primary measures in characterizing the plant canopy since it was found to be relevant to agricultural yields (Watson 1947). LAI can be measured with direct methods, such as harvesting or litter collection (Jonckheere et al. 2004), but these methods are time consuming and sometimes destructive to plants. For these reasons, in situ LAI is often determined with optical methods. From the theoretical viewpoint, optical LAI determinations are the inversions of radiative transfer models. In practice, optical instruments, e.g., the hemisphere camera or the LI-COR LAI2000 Plant Canopy Analyser (Welles and Norman 1991), are often used to measure gap fraction; then, based on statistic models about the leaf spatial arrangement, LAI is derived from measured light penetration (Monsi and Saeki 1953; Weiss et al. 2004). With the development of the technique, these methods can even be easily applied on forest canopies, which are normally out of reach from the ground.

Although optical LAI determinations are common, they also have some drawbacks. Due to the conical field of view of the instruments, optical LAI is just a statistic average over a large 2D extension; or in other words, it is stand oriented. As a consequence, this average value can hardly be used to characterize the structure of a heterogeneous canopy that is quite common in the conifer or canopy-unclosed deciduous forest. Furthermore, since many eco-physiological models simulate physiological processes at the tree level today, advanced methods that can supply leaf

area information in such a scale are required. This is especially important for conifer–deciduous mixed forests, as conventional LAI determinations can only be applied to pure conifer or pure deciduous stands. On the other hand, LAI is often underestimated with optical methods (Chen et al. 1991). This is because the Poisson model, which is used to derive LAI from gap fraction, assumes a random canopy (Nilson 1971), but in reality leaves are clumped in different scales and, for a certain leaf area, a clumped canopy allows more light penetration. Therefore, the accuracy of LAI determination can be improved if it uses the gap fraction measured at a finer scale, as the clumping effects above that scale can be directly eliminated (Lang and Xiang 1986; Chen and Cihlar 1995). Another additional benefit for determining leaf areas at individual tree level is that the results can be directly verified with allometric equations, since they are also individual tree oriented and estimate 'true' leaf areas (Chen et al. 1997; Küßner and Mosandl 2000; Jonckheere et al. 2005).

For the above reasons, if leaf areas of individual trees can be directly determined with optical instruments, the technique will be enhanced on both resolution and precision aspects. In fact, some studies using quantum light sensors had been performed on orchard or bush trees (Lang and McMurtrie 1992; Villalobos et al. 1995; Brenner et al. 1995). The methods used in these studies were similar: first, the mean LAI of a tree was derived by measuring gap fraction; then, the volume of the crown, which was assumed to be of regular shape, was estimated through measuring the dimensions of the crown shadows; finally, the total leaf area of the tree can be obtained as the product of the mean LAI and the crown volume. Unfortunately, although acceptable accuracy was acquired when these methods were applied on low and isolated plants, they can hardly be used in actual forests. The reason is twofold. First, it is very difficult to obtain the gap fraction of individual trees in an actual forest, as the shadows of crowns on the light sensor usually overlap with each other. Second, because crowns in an actual forest are seldom in a regular shape and LAD within a crown is unlikely to be evenly distributed, local LAD and the relevant volume should be measured for calculating the leaf area; but conventional optical instruments are not competent for such tasks.

Compared to other optical instruments, laser scanners have the exceptional capability to record the distances between the scanners and targets that the laser shots hit. In addition, laser points from different scans can be displayed as an aligned point cloud in the 3D environment. These characters supply new opportunities in the determination of leaf areas. Leaf areas of young western larches represented by the number of laser returns was estimated by subtracting leaf-off laser returns from leaf-on returns (Clawges et al. 2007). Based on voxelization, the vertical leaf area profiles of broadleaved trees and canopies were examined by counting the contact frequency of the laser beams (Hosoi and Omasa 2006, 2007). Noticeably, it was found that advanced terrestrial laser scanners could also be used to measure the gap fraction (Lovell et al. 2003; Henning and Radtke 2006; Danson et al. 2007a).

In this study, a terrestrial laser scanner LMS-Z360 was used for estimating leaf areas of individual trees in a Norway spruce stand, where the highly clumped canopy demands methods that have a better performance in eliminating the clumping effect. At the same time, the discontinuity between crowns also makes the isolation of tree points much easier. The main idea was for each objective tree, using a single scan to measure local gap fraction beyond determined crown depths and combining this scan with other scans to delineate the geometrical dimensions of the crown. Then, by integrating the information from both aspects, the local leaf area density (LAD) and the corresponding volume can be derived. Finally, the total leaf area can be obtained as the scalar product of these two variables.

## Materials and methods

### Experimental plots

The method was tested in a long-term experimental stand Fürstenfeldbruck 612 (FFB 612), 40 km northwest of Munich, Germany (48°14′N, 11°05′E). FFB 612 is a pure, even-aged Norway spruce stand, which is located 550 m above the sea level, with mean annual temperatures of 7.5°C and mean annual precipitation of 825 mm. Trees were planted in the stand in 1974 when they were 4 years old. The stand was composed of 11 plots and each was 0.09-ha big. The test trees were chosen from two plots, numbered as Plot 1 and Plot 3. Plantation in Plot 1 was with a spacing of 2 m × 1.25 m. In 2006, the stem density was 1,198 trees/ha, the mean tree height was 19.3 m, the mean diameter at breast height (DBH) was 0.210 m and the basal area density was 41.62 $m^2$/ha. Plantation in Plot 3 was with a spacing of 1 m × 1 m. In 2006, the stem density was 1,989 trees/ha, the mean tree height was 18.8 m, the mean DBH was 0.171 m and the basal area density was 45.78 $m^2$/ha.

### Data acquisition

Eleven trees were randomly chosen for the test. Three trees of numbers 4, 5 and 6 were from Plot 3 and others from Plot 1. For trees from numbers 1–6, the laser data sets were acquired under a clear sky on 11 July 2008. For trees from numbers 7–11, the laser data sets were acquired under an

overcast sky on 4 November 2008. All laser data sets were acquired in a near windless condition. DBH of each tree was measured with a tape ruler on the same day of scanning. Heights of all trees were measured with Vertex IV (HAGLÖF Company, Sweden) on 12 February 2009.

The laser scanner used in this study is a 3D-Laser Mirror Scanner LMS-Z360 (RIEGL Company, Austria), which is a surface imaging system based on accurate distance measurement by means of time-of-flight measurement of short infrared laser pulses. It works on a two-axis beam scanning mechanism. Lines and frames are two dimensions of the scanning. Line scans are obtained through rotating the mirror and frame scans through rotating the optical head. The laser wavelength is 0.9 μm. For natural targets, the measurable range is from 2 to 200 m. The accuracy of distance measurement is 0.012 m. The divergence of the laser beam is smaller than 0.12° (or 2 mrad, which corresponds to 0.02 m beam width per 10 m), if it is focused to infinity.

For each tree, two scans were acquired on opposite positions around the objective tree (Fig. 1). The rotating axis of the scanner head, i.e., $Z$ axis, was laid horizontally. $Y$ axis was also horizontal, but perpendicular to the $Z$ axis and pointed to the objective tree. $X$ axis was perpendicular to the $YZ$ plane and pointed to the ground. The range of line scan angle ($\theta$) was from 50° to 140°, with $Z$ axis as 0° and $-Z$ axis as 180°. The range of frame scan angle ($\varphi$) was from 90° to 270°, with $X$ axis as 0° and $-X$ axis as 180°.

Only the first return of each laser shot was recorded. The laser beam was focused to 20 m. In such a setting, if angle step widths were set as 0.12° for both line and frame scans, it would be the 'Panorama' scan pattern. It means that the laser spots on the object surface are side by side, without either overlapping or gaps. But it was found that if angle step widths of pixels were as big as angle step widths of laser shots, there would be blank strips on the generated range images. This should be due to the performance of the scanner, since most strips were found at the edges of branches and stems. Such noise could be sufficiently eliminated when smaller angle step widths of laser shots were used in scanning for certain angle step widths of pixels. In this study, angle step widths of pixels in range images were set as 0.12°, so angle step widths for both line and frame scans were set as 0.10°.

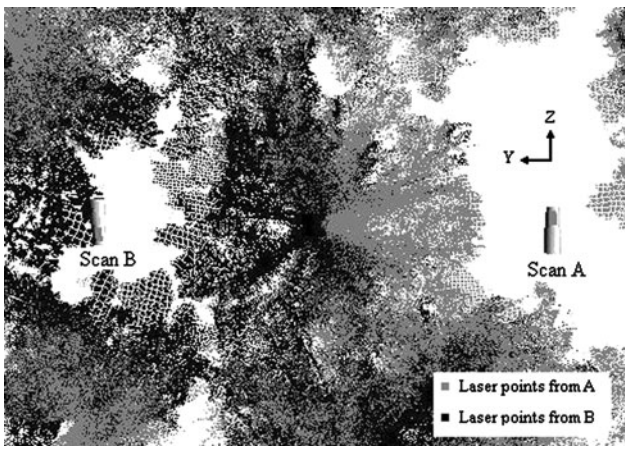


**Fig. 1** *Top view* of the aligned point cloud around tree number 3. Two laser data sets acquired around tree number 3 are aligned. Then, they are put in a scene under the orthogonal perspective mode and viewed from top. Scans *A* and *B* show the scanning positions. *Gray points* belonged to Scan *A*. *Black points* belonged to Scan *B*. The *Y* and *Z* axes show the corresponding scanning axes of Scan *A*

During scanning, five reflectors were put under the tree and scanned as tie points for registration. Snapshots of the scene covered by laser scanner were also acquired afterward with a calibrated Nikon D70 camera (Nikon Corporation, Japan), which was mounted on the scanner head.

## Objective tree isolation

One scan was chosen arbitrarily as the main scan, namely Scan A, which would be used to measure gap fraction. The other, namely Scan B, was referenced to Scan A. Then, the origin of Scan A became the coordinate origin of all laser points. The registration was performed by the RiSCAN Pro software. The standard deviations of corresponding tie points were smaller than 0.002 m.

Following this, the laser points were assigned colors from snapshots. It was found that some laser points have the color of the sky. This indicated that those points were at positions where there should be the gaps and should be no return signals. It was considered that such mistakes were due to the big divergence of laser beams (Danson et al. 2007b). For solving this problem, those false points, which were recognized as their blue channel was above a certain value, were eliminated from the data sets.

After the above processing, points belonging to the objective tree were extracted from the aligned 3D point cloud with visual inspection (Fig. 2) and stored as two data sets: Data set A, which included points only from Scan A; Data set $A + B$, which included points from both scans.

## Range image generation

For each tree, two range images, $A$ and $A + B$, were created as cylindrical projections of two data sets, respectively (Fig. 3a). In the range image, the range of each laser shoot was stored across red, green and blue channels of the corresponding pixel. Before the projection, all pixels were set in white color, which represents an empty pixel. The projection was implemented as the coordinate system transformation. First, the coordinates of laser points were transformed from the Cartesian coordinate system ($x$, $y$ and

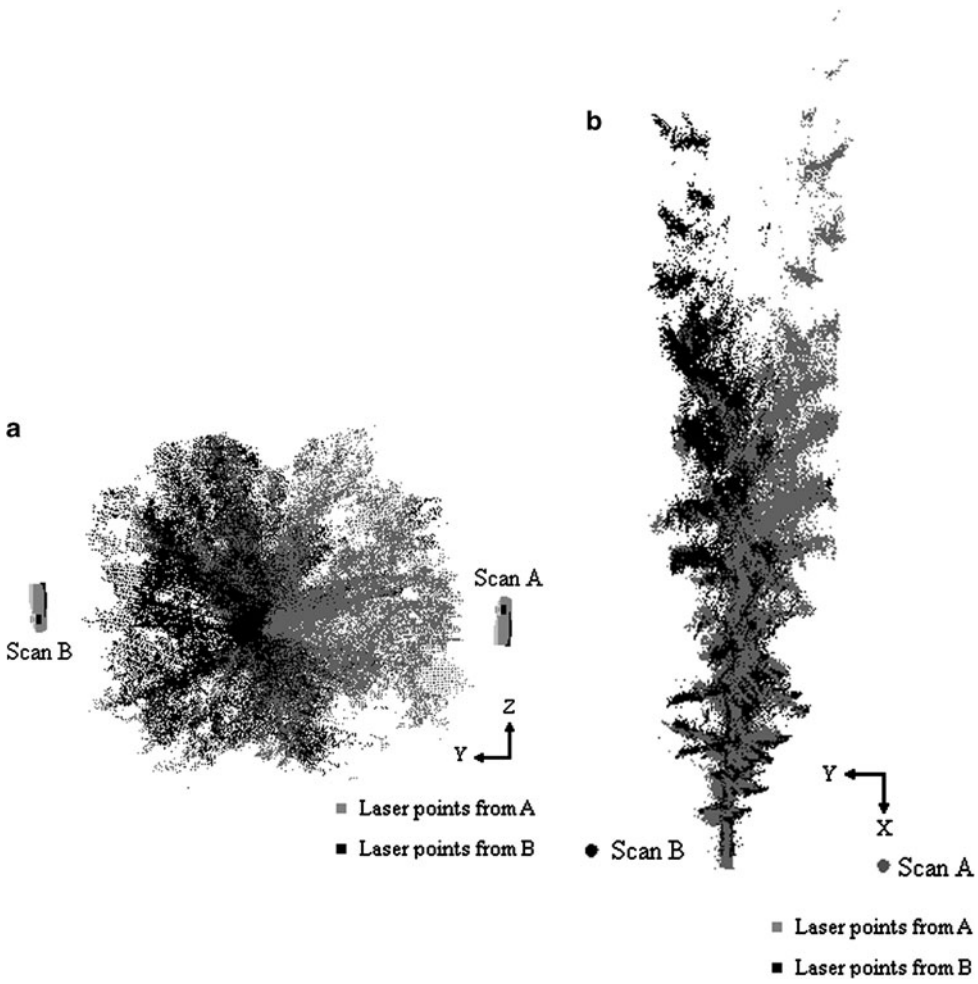


**Fig. 2** **a** *Top view* of isolated points belonging to tree number 3. The points belonging to tree number 3 are isolated from two laser data sets through visual inspection. The points are put in a scene under the orthogonal perspective mode and viewed from top. **b** *Side view* of isolated points belonging to tree number 3. The isolated points are put in a scene under the orthogonal perspective mode and viewed from the direction perpendicular to the *XY* plane of Scan *A*

$z$) to the spherical coordinate system ($\theta$, $\varphi$); then, they were further transformed to the image coordinate system ($v$, $u$). The pixel [0, 0] corresponded to $\theta = 50°$, $\varphi = 90°$ and each pixel corresponded to an angle step width of 0.12°, so the transformation functions were

$$v = \left(90 - \arctan\left(z \Big/ \sqrt{x^2+y^2}\right) - 50\right) \Big/ 0.12, \quad \text{for } z > 0, \tag{1}$$

$$v = \left(90 - \arctan\left(-z \Big/ \sqrt{x^2+y^2}\right) - 50\right) \Big/ 0.12, \quad \text{for } z < 0 \tag{2}$$

and

$$u = (90 - \arctan(y/-x))/0.12, \quad \text{for } y > 0, \tag{3}$$

$$u = (90 + \arctan(-y/-x))/0.12, \quad \text{for } y < 0. \tag{4}$$

According to the above functions, the distortion was introduced into the angle width along the $U$ axis. But this was neglected, since the line scan angles were near 90° ($50° < \theta < 140°$) and between this scope the distortion should be trivial. For either image, there could be more than one laser point corresponding to a pixel. In the single-scan image, the distance of the point latest processed was assigned to the corresponding pixel. In the dual scan image, the distance of the farthest point was recorded. After the projection, the trunk part, discriminated with visual inspection, was cut off in the single-scan image.

## LAD and volume derivation

If an objective tree had been laid horizontally, the tree crown could be deemed as a horizontally extending "canopy". The two range images could be deemed as two range-recording 'photographs' taken below and above this single-crown 'canopy'. Under such an analogy, the principle and methodologies of traditional optical LAI determinations can be applied to this study.

Along the trunk direction, the thickness and LAD of this single-crown 'canopy' were not homogeneous (Fig. 2b). For dividing this 'canopy' into homogeneous blocks, analogous to conventional LAI determinations (Lang and Xiang 1986; van Gardingen et al. 1999), two range images were plotted into segments. Each segment was composed of $L \times W$ pixels, where $L$ and $W$ are the line and frame

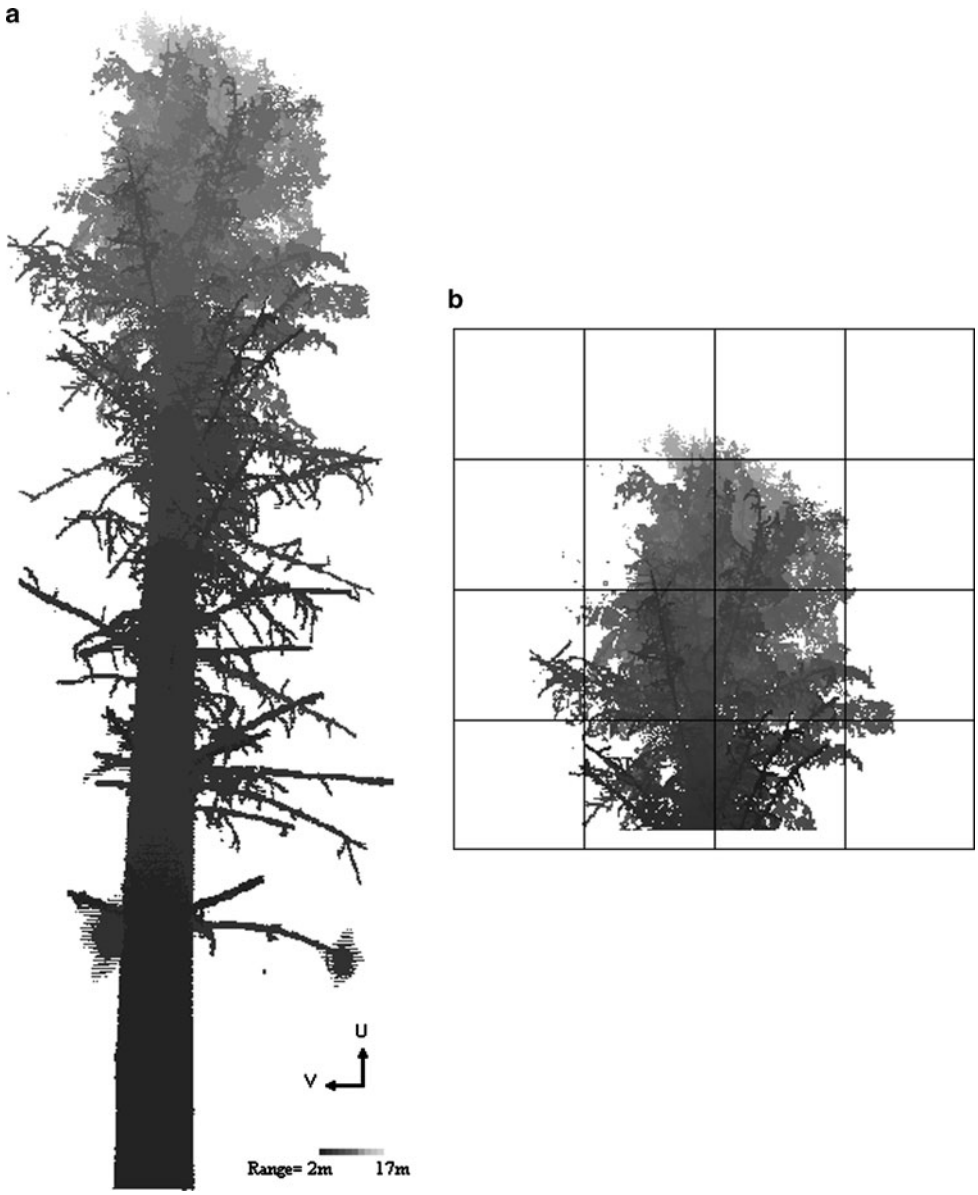


**Fig. 3** **a** Single-scan range image of tree number 3. The picture is a range image of tree number 3. It is obtained through projecting the laser points of data set A with a cylinder projection. The *gray values* represent the distance from the scanner, with white indicating the empty pixels. In real processing, distance-coded false color images were used. **b** Segmented crown range image of tree number 3. The crown part of tree number 3 was extracted out and plotted into segments. Each segment has 80 × 80 pixels. The *black straight lines* show the boundaries of segments

numbers (Fig. 3b). Thus, two segments, which were from different images ($A$ and $A + B$) but in the same position, formed a segment pair. The segment from the single-scan image was named Segment $A$ and that from the dual scan image was named Segment $A + B$.

In the 3D space, a segment pair corresponds to a radial square pyramid, the apex of which is at the origin of Scan A (Fig. 4). As only the first return of each shot was recorded by the scanner, it was assumed that all needles in the pyramid were encapsulated between two spherical surfaces, the radii of which equaled to ranges of the closest pixel in Segment A and the farthest pixel in Segment $A + B$, respectively. For the convenience of discussion, this space is called the needle space. It follows that the leaf area in this space would be determined under the assumption that shoots were randomly distributed in it.

In this study, leaf area was obtained as the product of LAD and the volume. Then, LAD can be obtained as the ratio between LAI and the 'canopy' height (Norman and Welles 1983). Furthermore, LAI can be derived by analyzing the gap fraction measured on Segment $A$. The volume of the needle space can be determined with the radii of the two spherical surfaces.

Usually, gap fraction can be calculated as the ratio between the sky pixel number and the total pixel number. But as crowns of Norway spruce were very dense, gap fractions of some segments would equal to zero under such a definition. For solving this problem, the gap beyond a

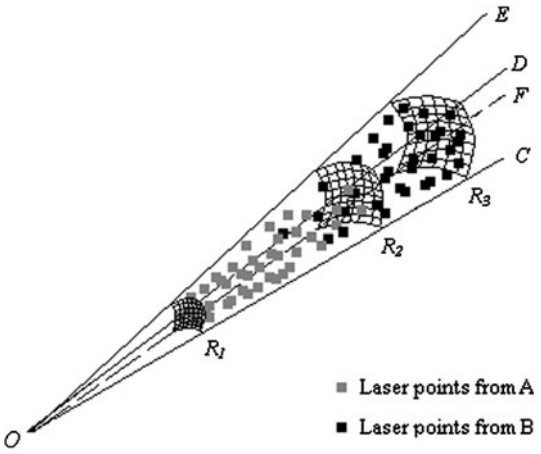


**Fig. 4** The virtual 3D view of the space corresponding to a segment pair. *O* is the origin of Scan A. *O-CDEF* is a radial square pyramid. $R_1$ and $R_2$ are ranges of the nearest and farthest pixel in segment A to *O*. $R_3$ is the range of the farthest pixel in segment $A + B$ to *O*. The mash nets represent the in-pyramid parts of three spheres, which have *O* as the center and pass, respectively, $R_1$, $R_2$ and $R_3$. In the pyramid, the space between $R_1$ and $R_3$ is the needle space

certain range from the scanner was measured and this range was determined as

$$R = R_1 + (R_2 - R_1)p \quad (0 < p < 1) \tag{5}$$

where $R_1$ and $R_2$ are ranges of the nearest and farthest pixel in segment A, respectively; $p$ is a factor, which scales the sampling depth between $R_1$ and $R_2$ for detection of the gap fraction. The selection of a proper $p$ value will be analyzed later. Then,

$$P_{0R} = \frac{N_R + N_E}{L \times W} \tag{6}$$

where $P_{0R}$ is the gap fraction beyond the range $R$ in a particular segment A, $N_R$ equals to the number of pixels whose distances to the scanner are bigger than $R$ and $N_E$ equals to the number of empty pixels.

It should be noticed that empty (or white) pixels in a segment could include two kinds of pixels. One kind belonged to real gaps, where laser shoots had no returns. The other kind was just noise involved in the range image, as the scope of the range image had a regular shape and was set bigger than the projection of laser points. Despite all empty pixels surrounded by leaf (or color) pixels should be classified as gap pixels, there was not an easy way to discriminate these two kinds of pixels from each other. At the same time, although the involvement of noise pixels would lead to an overestimation of gap fraction, it also increased the volume of the needle space as compensation. For these reasons, the total number of empty pixels was used in Eq. 6.

Since all laser beams in the needle space were perpendicular to the spherical boundaries, it was guaranteed that these beams would have equal path length between ranges $R_1$ and $R$, if they could reach $R$. Including the above assumption about shoot random distribution, the preconditions for using gap fraction to derive LAI were satisfied (Nilson 1971; Welles and Norman 1991). As light interception by a coniferous canopy is determined by the shoot silhouette (projected along the laser beam direction) area of the canopy rather than the needle silhouette area, it can be obtained that

$$\mathrm{LAI}'_R = -\ln P_{0R} \tag{7}$$

where $\mathrm{LAI}'_R$ is the 'effective' shoot area index within $R$.

Because the "cos$\theta$" correction in the traditional optical LAI equation is not used in Eq. 7, $\mathrm{LAI}'_R$ is not accumulated on the vertical direction, but on the beam direction. Similar to conventional optical LAI determinations, $\mathrm{LAI}'_R$ should be corrected considering the shoot angle distribution (Ross 1981; Campbell and Norman 1989), clumping effect (Lang and Xiang 1986; Chen and Cihlar 1995) and involved woody area.

In this study, the conifer leaf area is defined as the spherical average (rotated about the longitudinal axis) of vertically projected needle area when the needles are detached and laid out flat horizontally (Stenberg et al. 1995). It should be noticed that, unlike the definition used by Riederer et al. (1988), the projected needle area used here is the average of the silhouette area for a whole rotation about the longitudinal axis of needles. This definition considered that needles could lie horizontally in their "nature" position when they were measured on the planimeter. Under such a definition, the ratio of the total surface area to the projected needle area is $\pi$ (Grace 1987). Stenberg et al. (1994) suggested that for conifer canopies, the $\overline{\mathrm{STAR}}$ (i.e., the ratio of spherically averaged shoot silhouette area to total needle surface area) can be used to correct indirect estimates of leaf area index based on light penetration. But for consistency with the leaf area definition used in this study, the $\overline{\mathrm{SPAR}}$ (i.e., the ratio of spherically averaged shoot silhouette area to the spherical average of the vertically projected needle area when the needles are detached and laid out flat horizontally) was used as the correction factor. Based on the assumption that shoots had spherical angle distribution,

$$\mathrm{LAI}_R = (1 - \alpha)\ \mathrm{LAI}'_R / \overline{\mathrm{SPAR}} \tag{8}$$

where $\mathrm{LAI}_R$ is the vertically projected needle area index within the range $R$ and $\alpha$ is the woody-to-total area ratio (Chen et al. 1997). Here, an empirical value of 0.1 was used as $\alpha$ (Homolová et al. 2007; Stenberg et al. 1995); an empirical value of 0.5 was used as $\overline{\mathrm{SPAR}}$, which was obtained from a 30-year-old non-treatment Norway spruce stand established in northern Sweden (Stenberg et al. 1995).

As above-mentioned, LAD can be obtained as the ratio between LAI and the 'canopy' height. In this study, the

'canopy' height for a needle space should be the distance between two boundary spherical surfaces. But since the gap was measured beyond the range $R$, the 'canopy' height should be the difference between $R$ and $R_1$. Then, it can be obtained that

$$\mathrm{LAD_s} = \mathrm{LAI'_R}/(R - R_1) \tag{9}$$

where $\mathrm{LAD_s}$ is the leaf area density between $R_1$ and $R$. As shoots were assumed to be randomly distributed in the needle space, $\mathrm{LAD_s}$ was also used as the leaf area density of the needle space.

For the volume of the needle space,

$$V_s = 0.002^2 LW\frac{R_3^3 - R_1^3}{3} \tag{10}$$

where $V_s$ is the volume of the needle space and $R_3$ the range of the farthest pixel in segment $A + B$. Then

$$\mathrm{LA_s} = \mathrm{LAD_s}V_s \tag{11}$$

where $\mathrm{LA_s}$ is the leaf area of the segment pair. The total leaf area of the objective tree can be obtained through summing up the leaf areas of all segment pairs:

$$\mathrm{LA}_n = \sum \mathrm{LA_s} \tag{12}$$

where $\mathrm{LA}_n$ is the total leaf area estimate of the objective tree. Because the laser data set of each tree was composed of two scans and any one of them could be used as the major scan, each tree had two estimates for its total leaf area. The average of the two estimates was used as the final result:

$$\mathrm{LA_a} = \overline{\mathrm{LA}_n}. \tag{13}$$

## Results

For each tree, the laser leaf area (LLA) was determined in 18 cases, which were implemented as combinations between three $p$ values ($p = 0.4$, 0.6 and 0.8) and six kinds of segment sizes ($L \times W = 10 \times 10$, $20 \times 20$, $40 \times 40$, $80 \times 80$, $160 \times 160$ and $320 \times 320$). As an example, the result obtained with $p = 0.8$, $L \times W = 80 \times 80$ is shown in Table 1.

The allometric leaf area (ALA) of each tree was also determined and used as the 'true' value to verify LLA (Table 1). To obtain ALA, the leaf biomass was first determined with an allometric equation developed by Seifert and Müller-Starck (2009), which was based on the data collected in southern Bavaria, Germany. The equation related the needle biomass of a Norway spruce quantitatively with its DBH and H:

$$\ln(\mathrm{BM}) = -2.4632 + 2.7573 \cdot \ln(100 \cdot \mathrm{DBH}) - 1.1194 \cdot \ln(H) \left(r^2 = 0.880\right) \tag{14}$$

where BM is the needle biomass. Furthermore,

$$\mathrm{LA_t} = \mathrm{BM} \cdot \mathrm{SLA} \tag{15}$$

where $\mathrm{LA_t}$ is the ALA of a particular tree, SLA the specific leaf area, $H$ the tree height. $SLA$ was set as 3.5 ($\mathrm{m^2\ kg^{-1}}$), which was an empirical value obtained from a 35-year-old Norway spruce plot, also situated in southern Bavaria, Germany (Pretzsch and Mette 2008).

For evaluating the influence of the $p$ value and the segment size on leaf area determinations, the correlations between LLA and ALA were analyzed (Fig. 5). The correlations were based on a linear model

$$\mathrm{LA_t} = \beta_0 + \beta_1 \cdot \mathrm{LA_a}. \tag{16}$$

Statistical coefficients of this model were examined (Table 2). It can be found that the relationships were significant or very significant (i.e., with a small or very small $P_r$) for $\beta_1$ in all cases, but they were not significant for $\beta_0$ in any case. For a certain segment size, $P_r$ decreased when $p$ increased. In cases of $L \times W = 10 \times 10$, $20 \times 20$ and $40 \times 40$, $\beta_1$ decreased when $p$ increased. In cases of

**Table 1** LLA estimated with $p = 0.8$, $L \times W = 80 \times 80$ and allometric leaf areas for 11 trees

Trees are arranged in decreasing order of allometric leaf areas

| Number of trees | Maximal segment LAD ($\mathrm{m^2/m^3}$) | Laser leaf area ($\mathrm{m^2}$) | Allometric leaf area ($\mathrm{m^2}$) | DBH (m) | $H$ (m) |
|---|---|---|---|---|---|
| 1 | 2.08 | 84.97 | 118.86 | 0.302 | 21.0 |
| 2 | 1.20 | 94.43 | 114.87 | 0.277 | 17.5 |
| 3 | 1.25 | 68.12 | 87.32 | 0.269 | 20.8 |
| 4 | 1.24 | 71.79 | 75.36 | 0.256 | 21.0 |
| 5 | 0.58 | 26.62 | 55.61 | 0.240 | 23.5 |
| 6 | 1.43 | 62.29 | 54.81 | 0.232 | 21.9 |
| 7 | 0.71 | 27.77 | 34.03 | 0.190 | 20.5 |
| 8 | 0.76 | 43.86 | 30.48 | 0.180 | 19.8 |
| 9 | 1.26 | 32.52 | 29.15 | 0.170 | 17.9 |
| 10 | 0.28 | 11.30 | 26.72 | 0.173 | 20.2 |
| 11 | 0.24 | 8.09 | 18.93 | 0.147 | 18.4 |

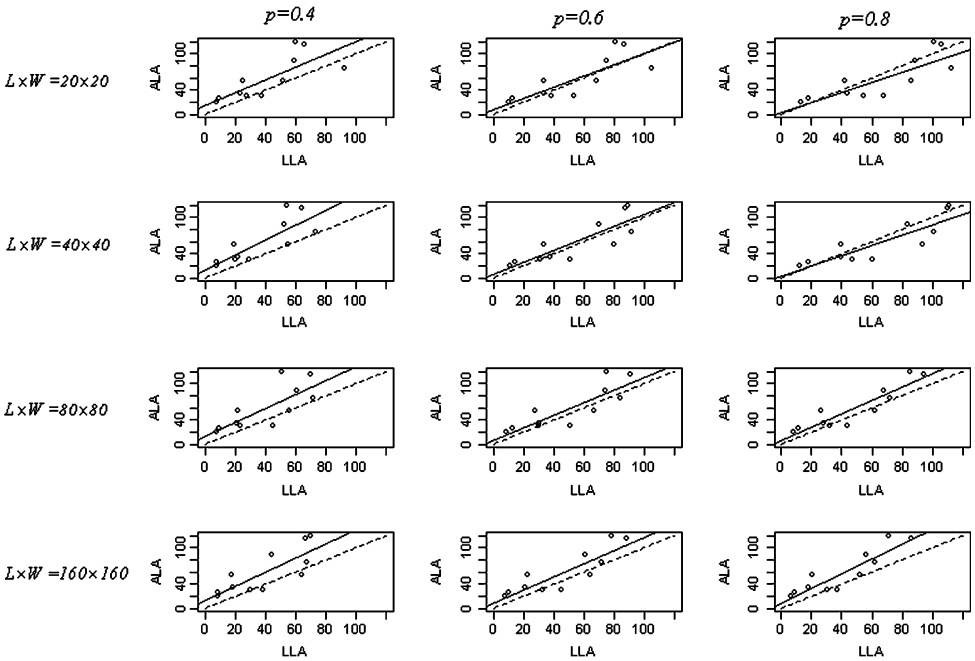


**Fig. 5** The correlations between LLA and ALA. LLA were derived under different combinations of $p$ and $L \times W$. Each *circle*, which represents a point at coordinates (LLA, ALA), corresponds to a tree. *Solid lines* show linear regressions fitted to the points. *Dashed lines* show the 1:1 relationship

**Table 2** Statistical parameters of correlations between LLA and ALA

| $p$ | $L \times W$ | $\beta_0$ | | | $\beta_1$ | | | $r^2$ |
|---|---|---|---|---|---|---|---|---|
| | | Estimate | $t$ value | $P_r$ (>\|$t$\|) | Estimate | $t$ value | $P_r$ (>\|$t$\|) | |
| 0.4 | 10 × 10 | 14.111 | 0.886 | 0.3986 | 0.899 | 3.210 | 0.0107 | 0.482 |
| | 20 × 20 | 15.363 | 1.080 | 0.3084 | 1.040 | 3.556 | 0.0061 | 0.538 |
| | 40 × 40 | 13.445 | 1.047 | 0.3225 | 1.232 | 4.129 | 0.0026 | 0.616 |
| | 80 × 80 | 13.063 | 0.892 | 0.3956 | 1.151 | 3.595 | 0.0058 | 0.544 |
| | 160 × 160 | 13.068 | 0.974 | 0.3555 | 1.160 | 3.961 | 0.0033 | 0.595 |
| | 320 × 320 | 12.962 | 0.920 | 0.3814 | 1.278 | 3.761 | 0.0045 | 0.568 |
| 0.6 | 10 × 10 | 10.029 | 0.640 | 0.5384 | 0.865 | 3.519 | 0.0065 | 0.532 |
| | 20 × 20 | 8.555 | 0.606 | 0.5595 | 0.923 | 4.050 | 0.0029 | 0.606 |
| | 40 × 40 | 5.285 | 0.408 | 0.6930 | 0.986 | 4.685 | 0.0011 | 0.677 |
| | 80 × 80 | 7.123 | 0.579 | 0.5768 | 1.031 | 4.811 | 0.0009 | 0.689 |
| | 160 × 160 | 8.705 | 0.792 | 0.4490 | 1.090 | 5.288 | 0.0005 | 0.730 |
| | 320 × 320 | 6.162 | 0.457 | 0.6583 | 1.438 | 4.428 | 0.0017 | 0.651 |
| 0.8 | 10 × 10 | 6.572 | 0.409 | 0.6918 | 0.772 | 3.639 | 0.0054 | 0.551 |
| | 20 × 20 | 3.014 | 0.207 | 0.8409 | 0.835 | 4.271 | 0.0021 | 0.633 |
| | 40 × 40 | 3.197 | 0.266 | 0.7965 | 0.851 | 5.229 | 0.0005 | 0.725 |
| | 80 × 80 | 5.487 | 0.594 | 0.5670 | 1.102 | 6.671 | 9.2e-05 | 0.813 |
| | 160 × 160 | 9.226 | 0.997 | 0.3449 | 1.212 | 6.299 | 0.0001 | 0.795 |
| | 320 × 320 | 4.526 | 0.347 | 0.737 | 1.782 | 4.700 | 0.0011 | 0.678 |

$L \times W = 80 \times 80$ and $160 \times 160$, $\beta_1$ had a 'v'-shaped trend when $p$ increased. In the case of $L \times W = 320 \times 320$, $\beta_1$ increased when $p$ increased. For a certain $p$ value, $P_r$ had a 'v'-shaped trend when the segment size increased, while $\beta_1$ mainly increased.

Unlike hemispherical photographs, as this method was single tree oriented, there would be empty pixels around the crown projections in the range image. With a bigger segment size, segments in the margin of the crown projection would include more empty (white) pixels as noise.

**Table 3** LLA of full segments, derived with four kinds of sub-segment sizes

| Number of segments | Laser leaf area ($m^2$) | | | |
|---|---|---|---|---|
| | $L \times W = 5 \times 5$ | $L \times W = 10 \times 10$ | $L \times W = 20 \times 20$ | $L \times W = 40 \times 40$ |
| 1 | 3.58 | 6.02 | 10.60 | 17.25 |
| 2 | 13.55 | 13.46 | 12.89 | 13.80 |
| 3 | 36.01 | 31.16 | 25.60 | 25.27 |
| 4 | 7.33 | 7.13 | 10.19 | 14.54 |
| 5 | 16.43 | 12.59 | 7.88 | 6.33 |

For examining the influence of the segment size on leaf area estimation excluding such an effect, leaf areas of five full segments that had a size of 40 × 40 were determined with different sub-segment sizes (Table 3). The $p$ value was set as 0.8. It could be found that estimated leaf areas had big variations with changed sub-segment sizes, but such variations had no significant trend with sub-segment sizes increase.

## Discussions

### Validation of the results

The accuracy of the allometric leaf areas was examined with another allometric equation, which was developed by Küßner and Mosandl (2000) in a mature Norway spruce stand of Erzgebirge in eastern Germany. The stand was called Ökologisches Meßfeld (ÖMF). Through correlating the leaf biomasses of 11 objective trees derived, respectively, with two allometric equations, a linear relationship can be obtained:

$$\mathrm{BM} = 1.36\mathrm{BM}k - 2.93 \; (r^2 = 0.952) \qquad (17)$$

where BM$k$ is the needle biomass derived with the ÖMF equation. From Eq. 17, it can be found that two leaf biomass data sets have a good linearity. The deviation of the slope from unity can be explained as the Bavarian stand, which was used to develop BM equation, had a faster growing speed. Considering that the testing stand of this study had a similar age and geographic condition as the Bavarian stand, Eq. 14 can be deemed as a good predictor of the leaf biomass.

For evaluating the accuracy of the estimation, the most common criterion is the equality between the results and the expected value. Under this standard, the result under $p = 0.6$, $L \times W = 40 \times 40$, should be the best determination, since its $\beta_1$ value was closest to unity. But, because empirical values were used in calculation as stand-specified multiplying factors, e.g., $\overline{\mathrm{SPAR}}$, $(1 - \alpha)$ and SLA, the proportion between LLA and ALA could be distorted. For this reason, the linearity between the estimated values and the expected values should be a better criterion. Obeying this idea, the $P_r$ value of $\beta_1$ should be used as the measure. Thus, the results under $p = 0.8$, $L \times W = 80 \times 80$ should be the best, since the smallest $P_r$ value was obtained in this case.

### Selection of the gap fraction range and the segment size

As LAD derived within a bigger range $R$ should be more representative for the whole needle space, it is natural that a bigger $p$ value should be preferred. This was also reflected by the result of the experiment. For this reason, it could be a better solution to look for the corresponding range of a fixed small gap fraction, instead of measuring gap fraction within a certain range as implemented here.

The selection of a proper segment size would be much more complicated. According to conventional LAI determinations, a smaller segment size should bring a more accurate and bigger estimate on LAI, since the leaf area in a smaller space is more likely to be randomly distributed. The only lower limitation for the segment size is that it should not be too small that the gap fraction in a segment equals to zero (Lang and Xiang 1986). Since gap fraction within a range was used to derive LAI in this study, such a limitation can also be lifted. Additionally, a smaller segment size would lead to less noise pixels involved in marginal segments and a more precise estimate on crown dimensions. So, it seems that a smaller segment size should be preferred. But such a prediction was contradictory to the experimental result, since the smallest $P_r$ value was obtained with a medium segment size. It should be noticed that the gap fraction measurement of the new method was implemented as pixel number counting, thus a smaller segment size means a smaller sampling number. The deficiency of sampling will cause a severe problem in the accuracy of LAI determination (Radtke and Bolstad 2001). In this study, the observable $P_{0R}$ value in Eq. 6 was limited between $1/(L \times W)$ and $1 - 1/(L \times W)$; so, if the segment size become smaller, the observable interval will likewise become smaller. This will degrade the accuracy of gap fraction measurement when the actual gap fraction is either very small or very large. Therefore, the selection of a proper segment size as a discrete number is the trade-off between spatial uniformity and sampling abundance and

needs delicate manipulation. For improving the accuracy, a possible solution could be using variable segment sizes; namely, a segment should be further divided when the size of its biggest white area is above a certain value. In this case, a gap size analysis (Chen and Cihlar 1995) in the segment would be required.

Other aspects concerning accuracy

For a better accuracy, there were some other aspects that could be improved. Based on the assumption that shoots were randomly distributed in each needle space, the measured LAD between $R_1$ and $R$ was used to predict LAD between $R$ and $R_3$. But it was found that for each tree, two estimates with different scans as the major scan could have a big variation (Fig. 6), which is more obvious for most big trees. This suggested that the above assumption can sometimes depart significantly from reality. For this reason, the average of two estimates was used as the final result and it sufficiently solved the problem. Thus, it is expected that more reliable results could be acquired if more scans were added in other cardinal directions around the objective tree and the estimated obtained with these as the major scan were added in for averaging. Furthermore, if more scans were collected in farther positions, the crown dimension can be more precisely delineated. This is especially important for the top part of trees.

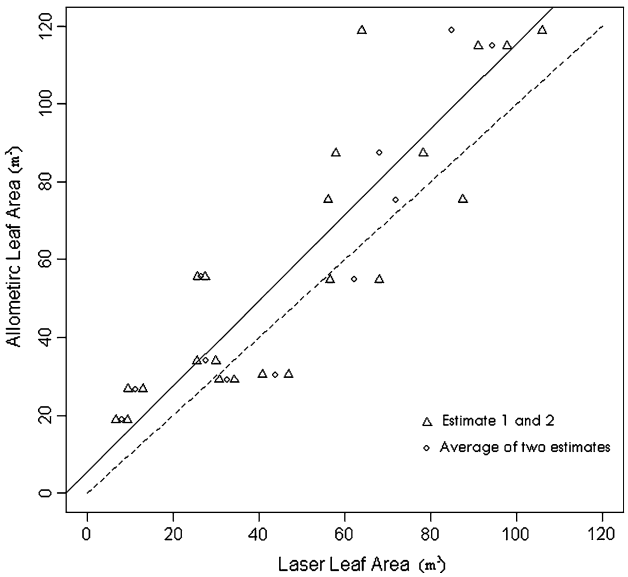


**Fig. 6** The correlation between LLA, estimated with $p = 0.8$, $L \times W = 80 \times 80$, and ALA. Each *circle*, which represents a point at the coordinates (LLA, ALA), corresponds to a tree. The *solid line* shows the linear regression fitted to the points. Two leaf area estimates of each tree, which use different scans as the major scan, are also shown in the graph with *triangles*. The *dashed line* shows the 1:1 relationship

At last, but not the least, if the laser beam divergence was reduced or full wave-form laser scanner was used, the gap fraction can be measured more precisely (Danson et al. 2008). This calls for a better performance of instruments.

## Conclusions

A new method using terrestrial laser scanner to estimate leaf areas of individual conifer trees was developed. The method was based on the theory of convenient optical LAI determinations, but further developed the technique in a 3D circumstance. With a proper gap fraction range and segment size, the testing estimates made in a mature forest stand were linear related and on average 10% lower than those acquired with an allometric equation. In future, the proper selection of the segment size depending on leaf size, tree height and spatial heterogeneity within individual crowns should be further studied. The influence of the $p$ value on the magnitude of estimates should also be examined considering non-randomness of the leaf area distribution and the beam divergence.

This method can be directly applied to actual forests. It should be very useful for heterogeneous, especially conifer–broad leaf mixed canopies. While extending the application of this method to deciduous forests, the technique of deriving leaf angle distribution with laser scanners needs to be developed.

## References

Brenner AJ, Cueto Romero M, Garcia Haro J, Gilabert MA, Incoll LD, Martinez Fernandez J, Porter E, Pugnaire FI, Younis MT (1995) A comparison of direct and indirect methods for measuring leaf and surface areas of individual bushes. Plant Cell Environ 18:1332–1340

Campbell GS, Norman JM (1989) The description and measurement of plant canopy structure. In: Russell G, Marshall B, Jarvis PG (eds) Plant canopies: their growth, form and function. Cambridge University Press, Cambridge, pp 1–19

Chen JM, Cihlar J (1995) Plant canopy gap-size analysis theory for improving optical measurements of leaf area index. Appl Opt 34:6211–6222

Chen JM, Black TA, Adams RS (1991) Measuring leaf area index of plant canopy with branch architecture. Agric For Meteorol 57:1–12

Chen JM, Rich PM, Gower ST, Norman JM, Plummer S (1997) Leaf area index measurements of boreal forests: theory, techniques, and measurements. J Geophys Res 102:29429–29443

Clawges R, Vierling L, Calhoon M, Toomey M (2007) Use of a ground-based scanning lidar for estimation of biophysical properties of western larch (*Larix occidentalis*). Int J Remote Sens 28:4331–4344

Danson FM, Hetherington D, Morsdorf F, Koetz B, Allgöwer B (2007a) Forest canopy gap fraction from terrestrial laser scanning. IEEE Geosci Remote Sens Lett 4:157–160

Danson FM, Giacosa C, Armitage RP (2007b) Two-dimensional forest canopy architecture from terrestrial laser scanning. In: Proceedings of the ISPRS Working Group VII/1 Workshop ISPMSRS'07:"Physical measurements and signatures in remote sensing". Davos, Switzerland

Danson FM, Armitage RP, Bandugula V, Ramirez FA, Tate NJ, Tansey KJ, Tegzes T (2008) Terrestrial laser scanners to measure forest canopy gap fraction. In: Hill RA, Rosette J, Suárez J (eds) In: Proceedings of SilviLaser 2008: 8th international conference on LiDAR applications in forest assessment and inventory, September 2008. Edinburgh, UK

Grace J (1987) Theoretical ratio between "one-sided" and total surface area for pine needles. N Z J Forest Sci 17:292–296

Henning JG, Radtke PJ (2006) Ground-based laser imaging for assessing three-dimensional forest canopy structure. Photogramm Eng Remote Sens 72:1349–1358

Homolová L, Malenovský Z, Hanuš J, Tomášková I, Dvoráková M, Pokorný R (2007) Comparison of different ground techniques to map leaf area index of Norway spruce forest canopy. In: Proceedings of the ISPRS Working Group VII/1 Workshop ISPMSRS'07: "Physical measurements and signatures in remote sensing". Davos, Switzerland

Hosoi F, Omasa K (2006) Voxel-based 3-D modeling of individual trees for estimating leaf area density using high-resolution portable scanning lidar. IEEE Trans Geosci Remote Sens 44:3610–3618

Hosoi F, Omasa K (2007) Factors contributing to accuracy in the estimation of the woody canopy leaf area density profile using 3D portable lidar imaging. J Exp Bot 58:3463–3473

Jonckheere I, Fleck S, Nackaerts K, Muys B, Coppin P, Weiss M, Baret F (2004) Review of methods for in situ leaf area index (LAI) determination Part I. Theories, sensors and hemispherical photography. Agric For Meteorol 121:19–35

Jonckheere I, Muys B, Coppin P (2005) Allometry and evaluation of in situ optical LAI determination in Scots pine: a case study in Belgium. Tree Physiol 25:723–732

Küßner R, Mosandl R (2000) Comparison of direct and indirect estimation of leaf area index in mature Norway spruce stands of eastern Germany. Can J For Res 30:440–447

Lang ARG, McMurtrie RE (1992) Total leaf areas of single trees of *Eucalyptus grandis* estimated from transmittances of the sun's beam. Agric For Meteorol 58:79–92

Lang ARG, Xiang YQ (1986) Estimation of leaf area index from transmission of direct sunlight in discontinuous canopies. Agric For Meteorol 37:229–243

Lovell JL, Jupp DLB, Culvenor DS, Coops NC (2003) Using airborne and ground-based ranging lidar to measure canopy structure in Australian forests. Can J Remote Sens 29:607–622

Monsi M, Saeki T (1953) Über den Lichtfaktor in den Pflanzengesellschaften und seine Bedeutung für die Stoffproduktion. Jpn J Bot 14:22–52 (On the factor light in plant communities and its importance for matter production. A new translation into English from German for the Annals of Botany with the permission of Professor Saeki, by M. Schortemeyer, vol 95, 2005, pp 549–567)

Nilson T (1971) A theoretical analysis of the frequency of gaps in plant stands. Agric For Meteorol 8:25–38

Norman JM, Welles JM (1983) Radiative transfer in an array of canopies. Agron J 75:481–488

Pretzsch H, Mette T (2008) Linking stand-level self-thinning allometry to the tree-level leaf biomass allometry. Trees 22:611–622

Radtke PJ, Bolstad PV (2001) Laser point-quadrat sampling for estimating foliage-height profiles in broad-leaved forests. Can J For Res 31:410–418

Riederer M, Kurbasik K, Steinbrecher R, Voss A (1988) Surface areas, lengths and volumes of *Picea abies* (L.) Karst. needles: determination, biological variability and effect of environmental factors. Trees 2:165–172

Ross J (1981) The radiation regime and architecture of plant stands. Springer, Berlin

Seifert T, Müller-Starck G (2009) Impacts of fructification on biomass production and correlated genetic effects in Norway spruce (*Picea abies* [L.] Karst.). Eur J Forest Res 128:155–169

Stenberg P, Linder S, Smolander H, Flower-Ellis J (1994) Performance of the LAI-2000 plant canopy analyzer in estimating leaf area index of some Scots pine stands. Tree Physiol 14:981–995

Stenberg P, Linder S, Smolander H (1995) Variation in the ratio of shoot silhouette area to needle area in fertilized and unfertilized Norway spruce trees. Tree Physiol 15:705–712

van Gardingen PR, Jackson GE, Hernandez-Daumas S, Russell G, Sharp L (1999) Leaf area index estimates obtained for clumped canopies using hemispherical photography. Agric For Meteorol 94:243–257

Villalobos FJ, Orgaz F, Mateos L (1995) Non-destructive measurement of leaf area in olive (*Olea europaea* L.) trees using a gap inversion method. Agric For Meteorol 73:29–42

Watson DJ (1947) Comparative physiological studies in growth of field crops. I. Variation in net assimilation rate and leaf area between species and varieties, and within and between years. Ann Bot 11:41–76

Weiss M, Baret F, Smith GJ, Jonckheere I, Coppin P (2004) Review of methods for in situ leaf area index (LAI) determination. Part II. Estimation of LAI, errors and sampling. Agric For Meteorol 121:37–53

Welles JM, Norman JM (1991) Instrument for indirect measurement of canopy architecture. Agron J 83:818–825